CHAPTER IV
RESULTS AND DISCUSSION

4.1 Synthesis of MCM-41

MCM-41 was synthesized by Microwave hydrothermal technique using MTAB (C14) and CTAB (C16) as templates. Figure 4.1 shows the XRD patterns of as-synthesized MCM-41. The XRD patterns of two different templates are similar, when compared with the reference pattern (see Figure 2.3), this result indicated that these materials are MCM-41. The peaks show typical three to four reflections between degree 2-theta at 2° and 5°. The reflections are due to the ordered hexagonal array of parallel silica tubes (as shown in Figure 2.4) and can be indexed a hexagonal unit cell as (100), (110), (200) and (210).

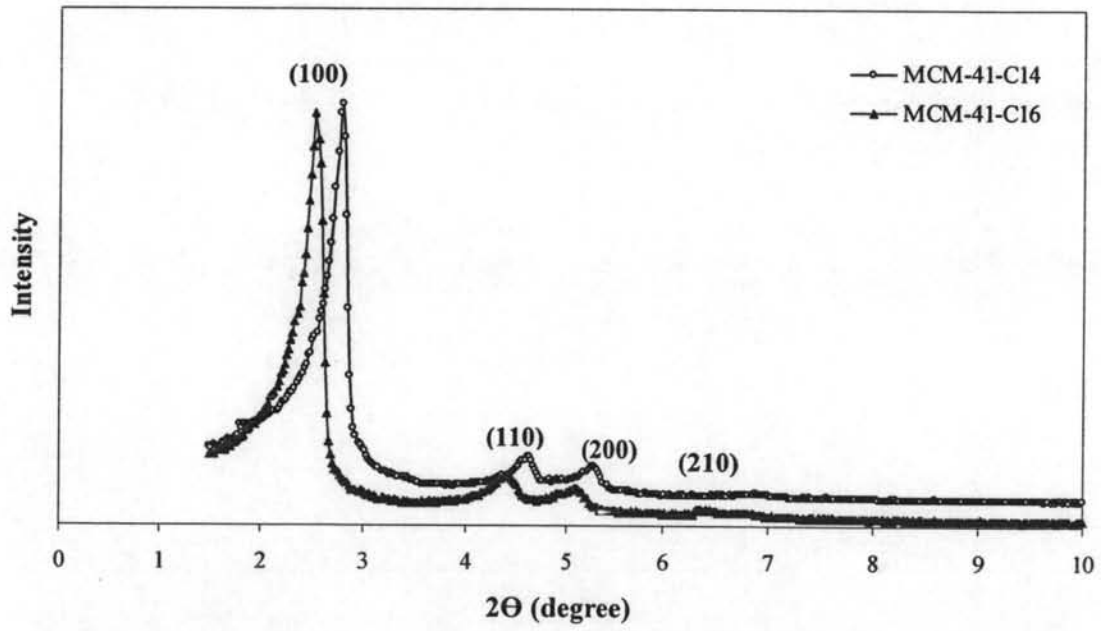

Figure 4.1 XRD patterns of as-synthesized MCM-41. (Prepared by using C14: MTAB and C16: CTAB.)

Due to the pore size diameter of MCM-41, the peak of MCM-41-C14 was shifted into higher degree. The pore diameter of as-synthesized MCM-41 depends on the nature of surfactant templates. Therefore, the longer hydrocarbon chain length of the surfactant template produced the bigger pore size of MCM-41 and increased spacing between pore to pore of hexagonal structure (Zhao *et al.*, 1996 and Selvam and Bhatia, 2001).

The structure of MCM-41, with MTAB (C14) as a surfactant template, was confirmed by TEM technique. From Figure 4.2, TEM image shows the uniform hexagonal array of mesoporous channels. This arrangement looks like a honeycomb. The evidences indicated that the synthesized samples are MCM-41.

Figure 4.2 TEM image of as-synthesized MCM-41-C14.

The physical properties of the as-synthesized MCM-41-C14 and MCM-41-C16 compared with KL-zeolite, which is supplied from Tosoh Co., Ltd. (Tokyo, Japan) are summarized in Table 4.1. Surface area and pore volume were obtained by a Quantachrome (Autosorb-1) following the BET procedure. All materials exhibited high surface areas (up to 1,200-1,400 m^2/g) and pore volume, excluding KL-zeolite.

Table 4.1 Physical properties of synthesized MCM-41-C14, MCM-41-C16 and commercial KL.

Description	MCM-41-C14	MCM-41-C16	KL-zeolite*
Surface area (m^2/g)	1,429	1,240	302
Pore diameter (Å)	25.50	36.90	7.10
Pore volume (cm^3/g)	0.99	0.96	0.21

* Commercial grade KL-zeolite was supplied from Tosoh Co., Ltd. (Tokyo, Japan).

4.2 Characterization of Fresh Catalysts

4.2.1 DRIFTS of Adsorbed CO

A DRIFTS of adsorbed CO has been used to characterize the location of Pt on KL-zeolite. For any catalyst supports, this technique can roughly examine the location of metal on the catalyst supports. Because the DRIFTS of adsorbed CO spectra depends on the stability of stretching frequency of CO adsorbed on Pt. Therefore, the other characterization techniques were required to specify the location of the metal on the catalyst support.

According to a report done by Stakheev *et al.* (1995), they revealed three criteria for interpretation of the location of Pt on KL-zeolite;

(a) Bands below 2050 cm^{-1} are assigned to Pt-CO species arising from the disruption of small Pt-clusters inside the zeolite channels.

(b) Bands between 2050 and 2075 cm^{-1} are associated with larger Pt-clusters in the near-surface region of the zeoloite.

(c) Bands around 2080 cm^{-1} are in general assigned to larger Pt-clusters in the external surface.

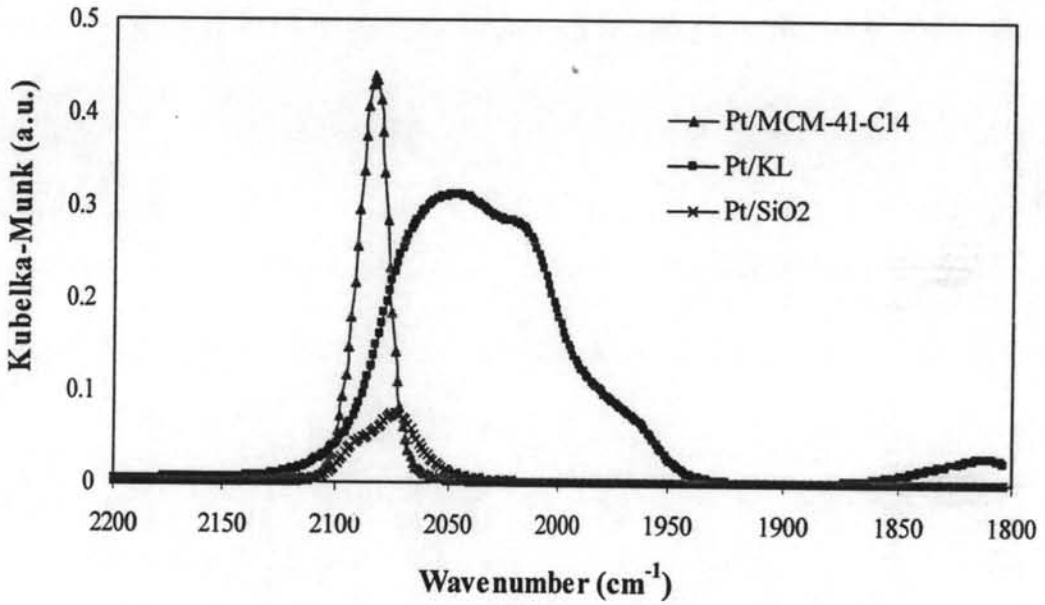

Figure 4.3 The DRIFTS spectra of adsorbed CO on 1% Pt/MCM-41-C14, 1% Pt/SiO_2 and 1% Pt/KL.

As shown in Figure 4.3, the DRIFTS spectra of CO adsorbed on 1% Pt/MCM-41-C14 prepared by VPI method and 1% Pt/KL prepared by VPI method. It is found that the spectra displays board band peak below 2050 cm^{-1}. This result could be interpreted that most of the Pt-clusters are small and located inside the zeolite channel with high dispersion. In contrast, the Pt supported on MCM-41-C14, the DRIFTS spectra shows a sharp peak around 2080 cm^{-1} which demonstrated that most of the Pt-cluster are located on external surface of the MCM-41 with bigger clusters than on KL-zeolite as observed on SiO_2.

4.2.2 TEM

TEM images of 1% Pt/MCM-41-C14 and 1% Pt/MCM-41-C16 show that the MCM-41 structure was not modified after Pt impregnation (Figures 4.4 (a) - 4.5 (a)). From Figures 4.4-4.5, the images show that the Pt-clusters were located on the external surface and these images could be indicated that the Pt-clusters sizes were about 5-25 nm.

Both TEM images of 1% Pt/MCM-41-C14 and 1% Pt/MCM-41-C16 presented the similar phenomena. After the reaction, the Pt-clusters are agglomerated to each other so it could be observed the Pt-clusters obviously. It should be noted that the reaction temperature (500°C) has affected to the mobility of Pt metal over MCM-41.

4.2.3 Hydrogen Chemisorption

Table 4.2 summarizes the H/Pt ratio of fresh catalysts. It can be seen that Pt/KL gave much higher H/Pt ratio than Pt/MCM-41 group. The result indicates that Pt/KL provided the highest Pt dispersion.

Table 4.2 Hydrogen chemisorption of the fresh catalysts.

Catalysts	**H/Pt**
1%Pt/MCM-41-C14	0.24
1%Pt/MCM-41-C16	0.17
1%Pt/SiO_2	0.08
1%Pt/KL	1.14

(a)

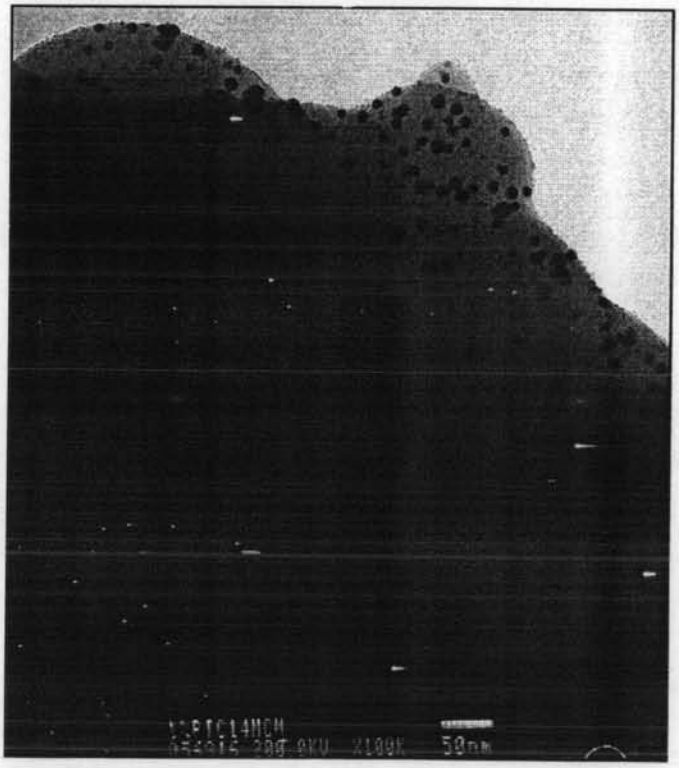

(b)

Figure 4.4 TEM image of 1% Pt/MCM-41-C14 (a) fresh catalyst (b) spent catalyst.

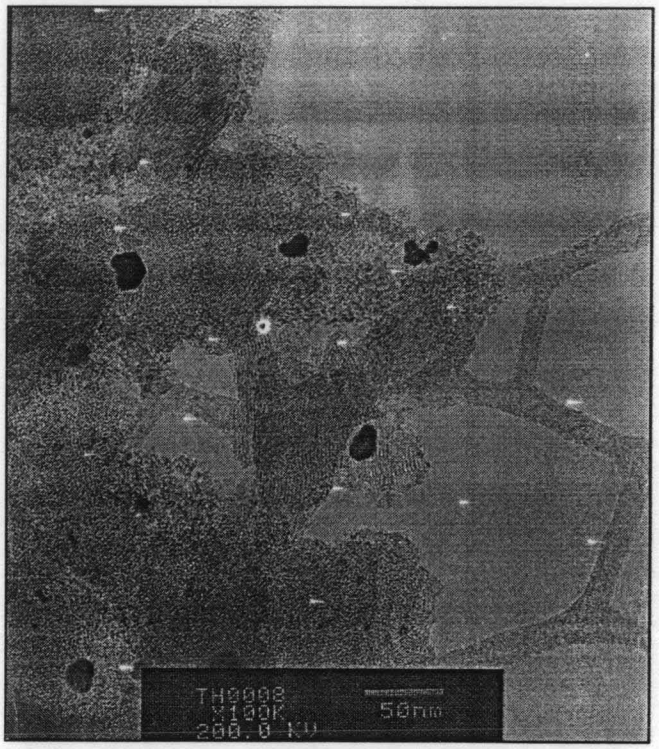

(a)

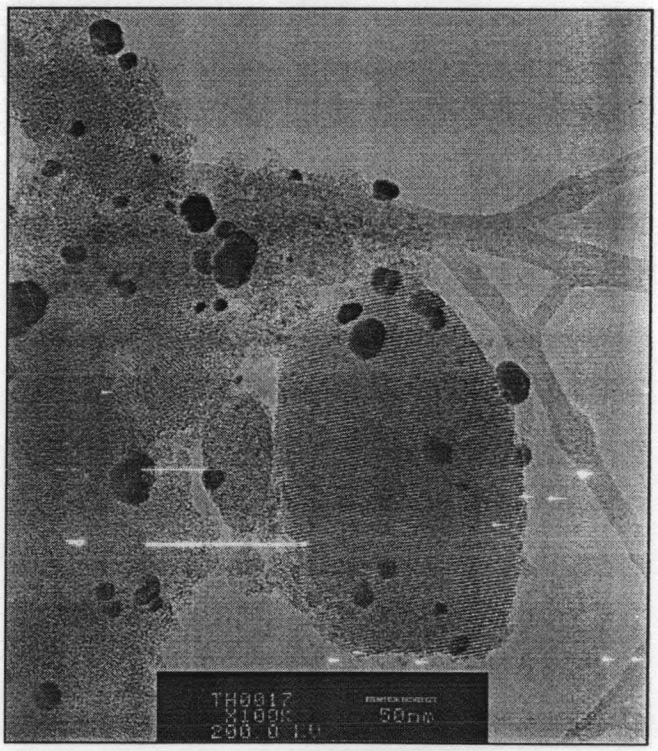

(b)

Figure 4.5 TEM image of 1% Pt/MCM-41-C16 (a) fresh catalyst (b) spent catalyst.

4.2.4 Temperature Programmed Reduction (TPR)

Figure 4.6 shows TPR profiles obtained on 1%Pt/MCM-41-C14, 1%Pt/MCM-41-C16 and 1%Pt/KL. These results show that two reduction curves are occurred. Its can be indicated that there are two species of Pt on the MCM-41 support. The first curve is due to the consumption of H_2 for the reduction of PtO to Pt, presented in low temperature range 90-170°C. And another curve is Pt_2O to Pt at high temperature range 300-420°C (Shen and Kawi, 2003). This phenomenon is same as 1%Pt/KL. But the high temperature reduction curve on the 1%Pt/KL presents at higher temperature range 380-480°C than both of 1%Pt/MCM-41. It indicates strong interaction of Pt on KL-zeolite.

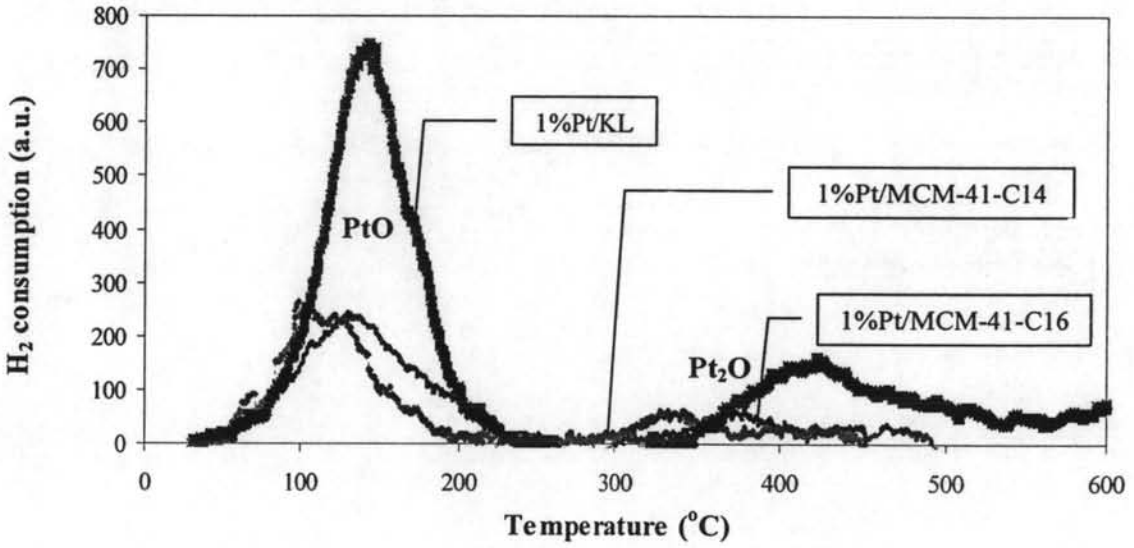

Figure 4.6 TPR profile for 1%Pt/MCM-41-C14, 1%Pt/MCM-41-C16 and 1%Pt/KL fresh catalysts.

4.3 *n*-Octane Aromatization Reaction

The catalysts with different pore sizes and different preparation methods (VPI and IWI) were tested for *n*-octane aromatization compared with Pt/KL and Pt/SiO_2 catalyst. The evidence of the conversion and the total aromatics are shown in Figure 4.7 and Figure 4.8, respectively. It was found that Pt/KL provided the highest conversion and total aromatics selectivity than other supports. For silica based support, Pt/MCM-41-C14 prepared by VPI method gave higher conversion than Pt/MCM-41-C16 and Pt/SiO_2. But Pt/SiO_2 gave total aromatics and C_8-aromatic selectivity much more than on MCM-41. Interestingly, at the initial time MCM-41 group exhibited high activity before quickly drop after 10 min time on stream and it showed high stability on conversion and total aromatics selectivity.

Furthermore, it was found that Pt/MCM-41-C14 prepared by IWI method provided in the lowest conversion and total aromatics selectivity. Therefore, it can be concluded that preparation methods have affected on the conversion and total aromatics selectivity.

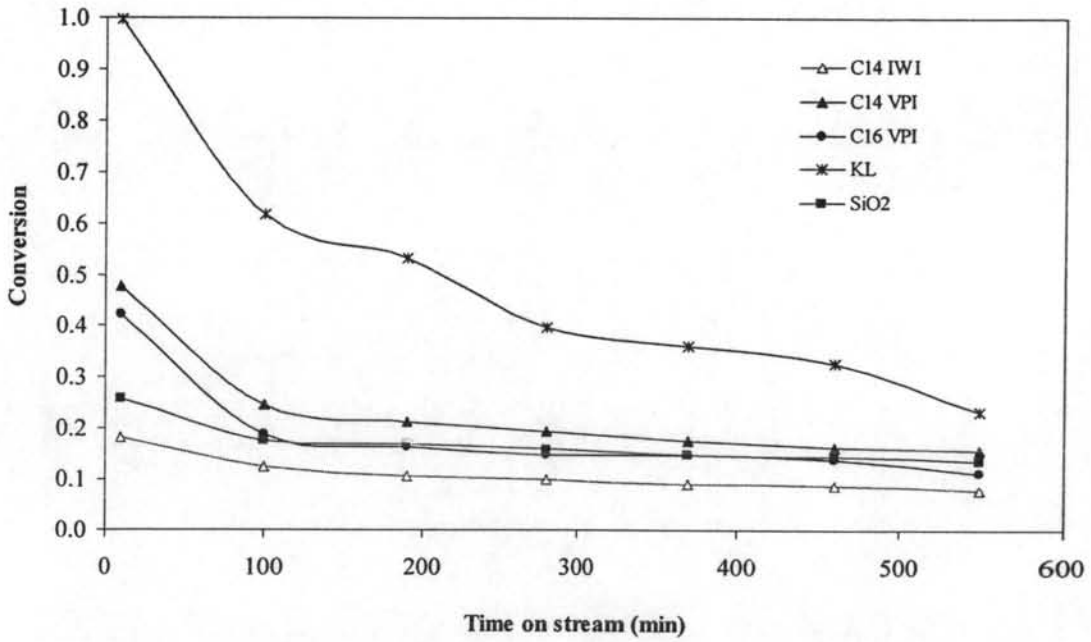

Figure 4.7 *n*-Octane conversion as a function of time on stream over Pt/MCM-41-C14 IWI, Pt/MCM-41-C16 VPI, Pt/MCM-41-C14 VPI, Pt/KL and Pt/SiO_2 catalysts.

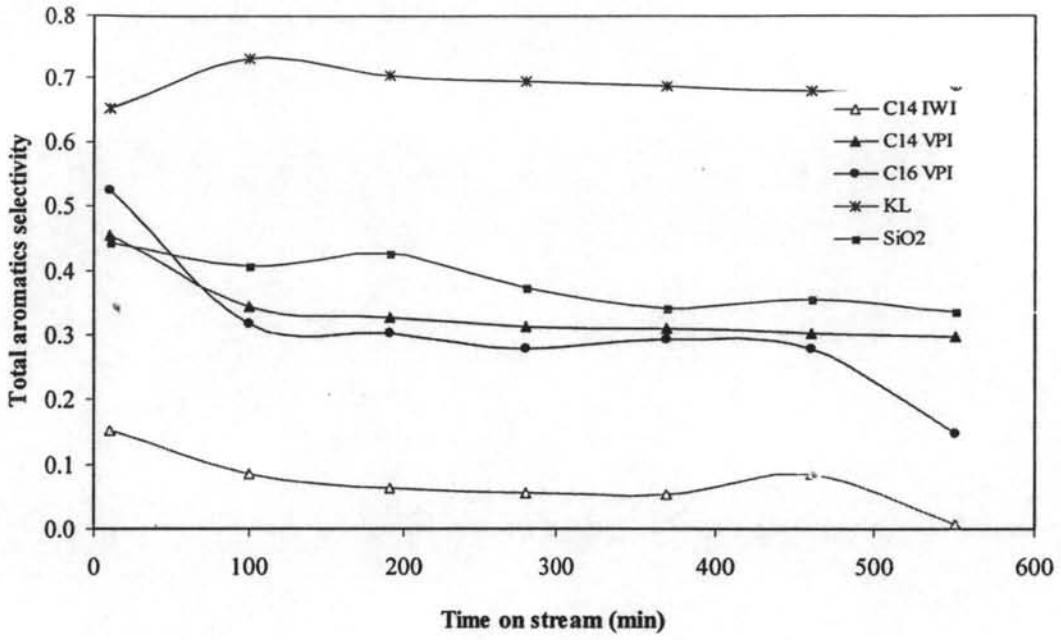

Figure 4.8 Total aromatics selectivity as a function of time on stream over Pt/MCM-41-C14 IWI, Pt/MCM-41-C16 VPI, Pt/MCM-41-C14 VPI, Pt/KL and Pt/SiO_2 catalysts.

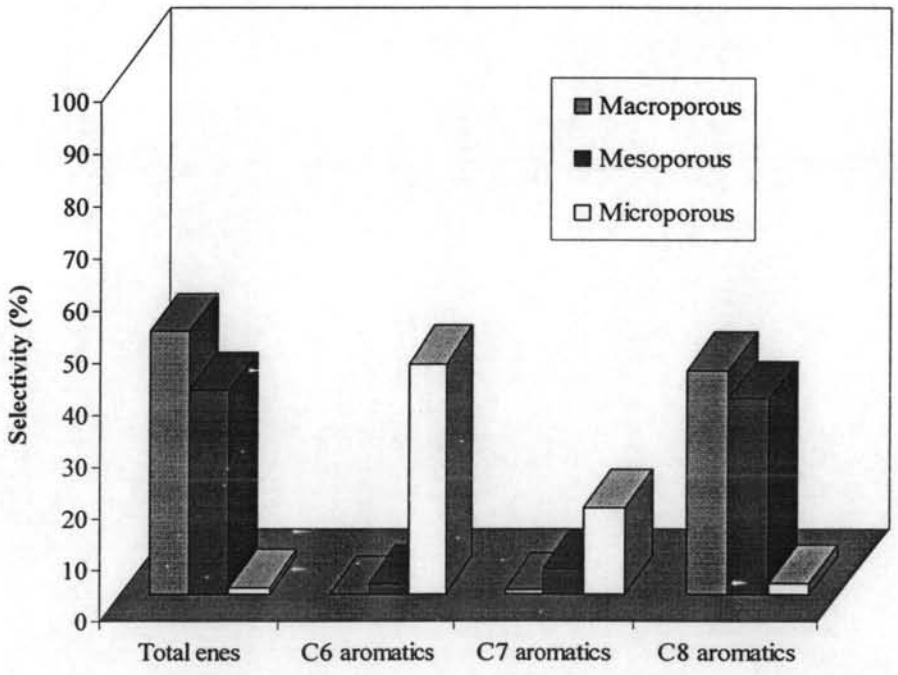

Figure 4.9 Product distribution of *n*-octane classified by type of the catalyst supports.

The product distributions obtained on the different catalyst are shown in Figure 4.9 and Table 4.3. It was illustrated that Pt/SiO_2 (macroporous) provided the highest selectivity value to C_8 aromatics and most of the aromatics product obtained are CX and EB. Whereas Pt/KL (microporous) gave low C_8 aromatic products similar as C14 IWI and most of the major aromatic products are benzene and toluene, which obtained from secondary hydrogenolysis reaction. Although low conversion found on Pt supported on MCM-41 (mesoporous), the aromatics obtained were C_8 aromatics as major products than on Pt/KL.

These results are in good agreement with H/Pt ratio. It might be due to Pt/KL has much more active surface area than on Pt/MCM-41 group. Therefore Pt/MCM-41 provided low conversion and less amount of coke.

In addition, it was found that the SiO_2-based supports, especially SiO_2 (macroporous) and MCM-41 (mesoporous), provided the high selectivity of total enes which are the aromatic intermediate. This is because there is no pore restriction on both supports. Therefore, the aromatic intermediates can diffuse freely through the pore channel without the interaction between the molecules and active sites leading to high selectivity of total enes and low conversion. Moreover, the C_8-aromatics on KL-zeolite (microporous) might undergo secondary hydrogenolysis reaction to benzene and toluene resulting in fewer amounts of C_8-aromatics (Jongpatiwut *et al.*, 2003).

Table 4.3 Product distribution of *n*-octane aromatization with 10 min time on stream. The reaction took place at 500°C, hydrogen to hydrocarbon ratio 6:1 and WHSV 5 h^{-1}

Product Distribution	***MCM-41***			***SiO_2***	***KL***
	Pt/C14-VPI	**Pt/C16-VPI**	**Pt/C14-IWI**	**Pt/SiO_2**	**Pt/KL**
Conversion	0.48	0.42	0.18	0.26	0.93
C1-C5	0.13	0.13	0.14	0.05	0.29
C6enes	0.30	0.28	0.59	0.37	0.01
Octenes	0.10	0.07	0.12	0.14	0.00
Benzene	0.02	0.02	0.01	0.00	0.45
Toluene	0.05	0.10	0.02	0.01	0.17
EB	0.13	0.13	0.04	0.17	0.02
m,p-Xylene	0.13	0.15	0.07	0.00	0.01
o-Xylene	0.12	0.13	0.03	0.27	0.01
Total aromatics	0.45	0.52	0.15	0.44	0.64
Total enes	0.39	0.35	0.71	0.51	0.01

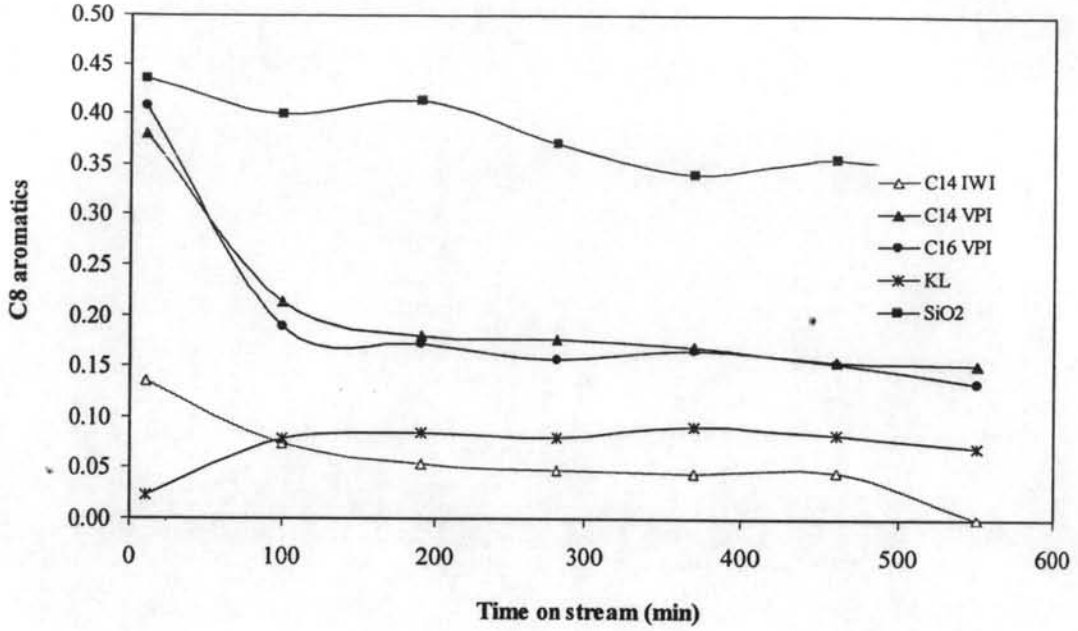

Figure 4.10 C_8-aromatics selectivity as a function of time on stream over Pt/MCM-41-C14 IWI, Pt/MCM-41-C16 VPI, Pt/MCM-41-C14 VPI, Pt/KL and Pt/SiO_2 catalysts.

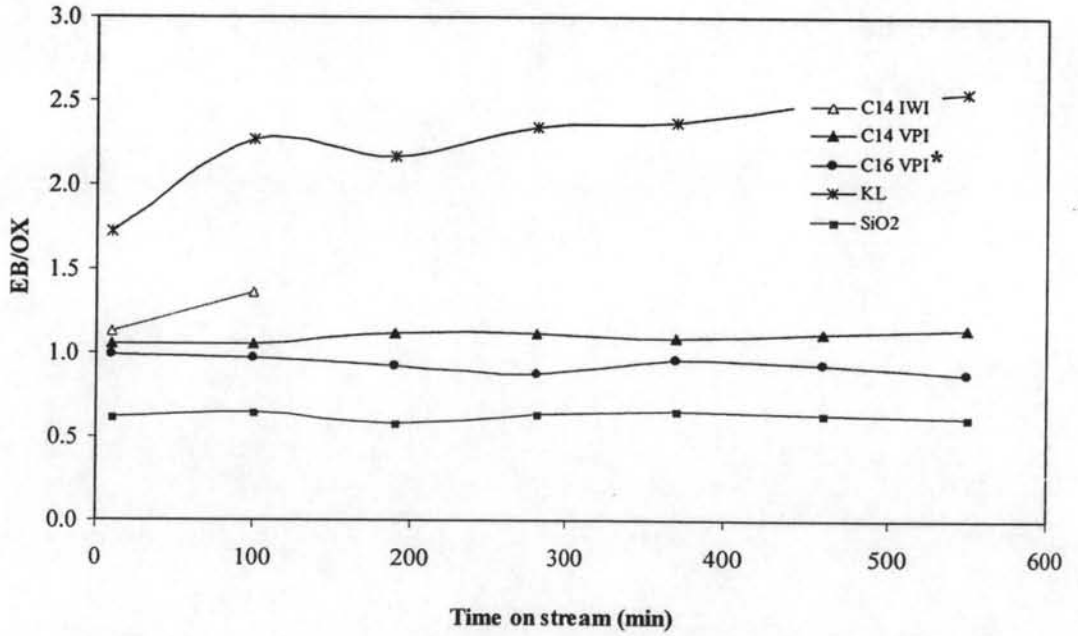

* C14 IWI, up to 100 min time on stream the OX product does not occurs

Figure 4.11 EB/OX ratio as a function of time on stream over Pt/MCM-41-C14 IWI, Pt/MCM-41-C16 VPI, Pt/MCM-41-C14 VPI, Pt/KL and Pt/SiO_2 catalysts.

From Figure 4.11, it was found that 1%Pt supported on KL-zeolite exhibited EB/OX ratio more than 1. Because the critical size diameter of OX is greater than that of EB and pore size of KL-zeolite. This facilitates secondary hydrogenolysis of OX to smaller molecules. C16 VPI and C14 VPI showed the EB/OX ratio value about 1.0, it could be implied that it was not transportation limit occurs because the pore sizes diameter of as-synthesized MCM-41 (as shown in Table 4.1) which have larger pore diameter than L-zeolite and than on the critical size of EB (6.7 Å) and OX (7.1 Å). Moreover, the EB/OX ratio of C16 VPI and C14 VPI remained constant.

4.4 Characterization of the Spent Catalysts

The amount of carbon deposited on spent catalyst after exposing to *n*-octane aromatization for 9 h on stream are summarized in Table 4.4. When comparing the amount of coke deposition on Pt/MCM-41. It was observed that the %coke deposit of both Pt/MCM-41-C14 and Pt/MCM-41-C16 are nearly the same. But the Pt/KL provided higher amount of coke than on Pt/MCM-41 group. Therefore, Pt/KL gave the highest conversion. Figure 4.7 of the TPO profile of both 1% Pt/MCM-41-C14 and 1% Pt/MCM-41-C16 are illustrated that this profile is the same trend.

Table 4.4 Amount of coke deposited on the spent catalysts, as determined by TPO, after the *n*-octane aromatization reaction 9 h on stream

Catalysts	%Coke deposit
Pt/MCM-41-C14	0.47
Pt/MCM-41-C16	0.38
Pt/KL	2.41

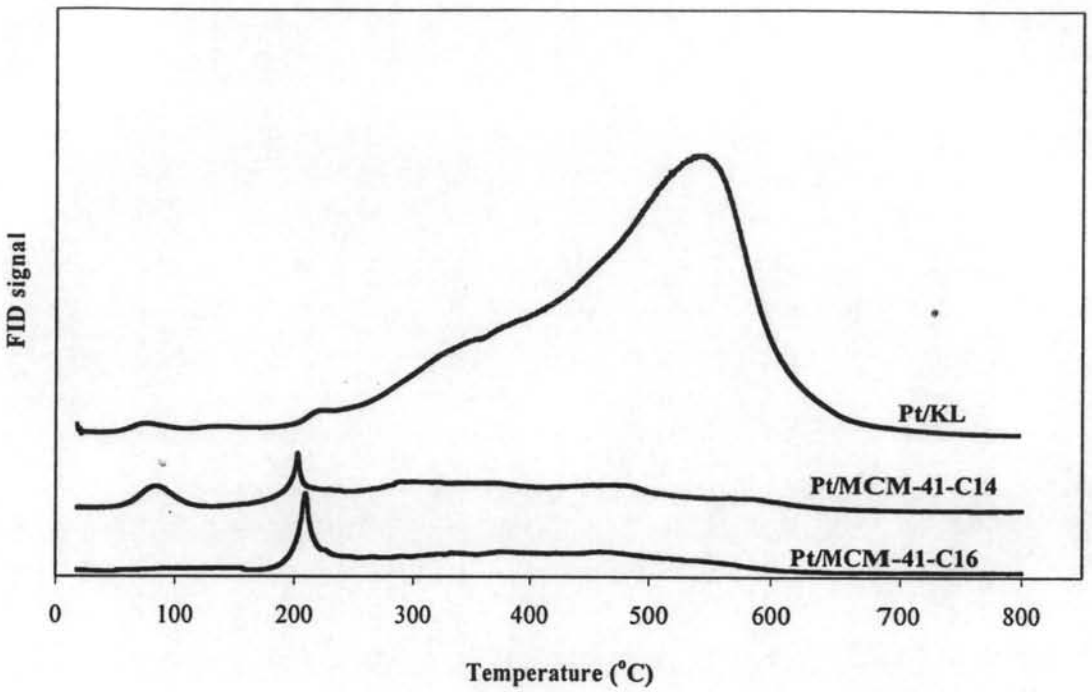

Figure 4.12 TPO profile for 1%Pt/MCM-41-C14, 1%PtMCM-41-C16 and 1%Pt/KL after 9 h on stream.

Moreover, Jongpatiwut *et al.* (2005) reported that in case of *n*-octane aromatization, the coke precursors are most probably the C_8 aromatic products, which slowly diffuse out from the support. The result can be explained in term of EB/OX ratio. It was found that Pt/MCM-41 group gave EB/OX ratio around 1.0 and provide low carbon deposit. It can be inferred that the transport limitation will be negligible for Pt/MCM-41 group.

By contrast, Pt/KL presented higher EB/OX ratio than on other supports. It can be implied that Pt/KL has an effect on transport limitation. Therefore it has higher amount of coke.